A novel oral dosage formulation of the ginsenoside aglycone protopanaxadiol exhibits therapeutic activity against a hormone-insensitive model of prostate cancer

Alain Gulenga Musende[a,e], Andy Eberding[a], Catherine A. Wood[a], Hans Adomat[a], Ladan Fazli[a], Antonio Hurtado-Coll[a], William Jia[c,d], Marcel B. Bally[b,e,f] and Emma S. Tomlinson Guns[a,f,g]

This study focuses on determining the pharmacokinetics, biodistribution, and efficacy of the ginsenoside aglycone protopanaxadiol (aPPD) administered as a single agent in a novel oral dosage formulation. To obtain these data and to characterize the stability of aPPD, appropriate analytical assay development was carried out. The solubility and stability of aPPD were determined, and the compound was formulated for oral gavage. aPPD levels in blood and tissues following oral administration to nu/nu nude mice were determined using liquid chromatography–mass spectrometry/mass spectrometry. The efficacy of aPPD was determined upon oral administration to nu/nu nude mice bearing PC-3 human prostate cancer xenograft tumors. Immunohistochemical analysis of tumor tissues was performed to establish apoptotic indices and Ki-67 expression as markers of proliferation. The maximum solubility of aPPD in ethanol was 68.4 mg/ml. aPPD administered at a dose of 70 mg/kg yielded a T_{max} of approximately 40 min and a C_{max} value of 3.9 ± 1.4 μg/ml, and no toxicity was observed. aPPD accumulated largely in the stomach and small intestine and was also present in the brain. This dose engendered a significant delay in PC-3 tumor growth, an increase in apoptotic index, and a decrease in Ki-67 levels. We have shown that aPPD is a stable compound that can be formulated for oral gavage. Pharmacokinetic studies demonstrate the ability of this compound to be absorbed after oral administration. Future studies will assess the activity and pharmacokinetics of aPPD when administered in combination with standard chemotherapy. ***Anti-Cancer Drugs*** **23:543–552 © 2012 Wolters Kluwer Health | Lippincott Williams & Wilkins.**

Anti-Cancer Drugs 2012, **23**:543–552

Keywords: biodistribution, efficacy, ginsenoside, pharmacokinetics, prostate cancer

[a]The Prostate Centre at Vancouver General Hospital, [b]Department of Advanced Therapeutics, British Columbia Cancer Agency, [c]Department of Surgery, [d]Brain Research Center, [e]Department of Pathology and Laboratory Medicine, [f]Faculty of Pharmaceutical Sciences and [g]Department of Urologic Sciences, University of British Columbia, Vancouver, British Columbia, Canada

Correspondence to Dr Alain Gulenga Musende, PhD, The Prostate Centre, Vancouver General Hospital, 2660, Oak Street, Vancouver, BC, Canada, V6H 3Z6
Tel: +1 613 979 6744; fax: +1 604 875 5654; e-mail: alainmus@gmail.com

Received 29 July 2011 **Revised form accepted** 5 December 2011

Introduction

It is known that cancer patients often take complementary and alternative medicines while being treated with the best available treatment options [1]. Most patients consider use of complementary and alternative medicines because they feel the product will not do harm, based on an assumption of lack of toxicity [1], while also providing potential therapeutic benefits. As one example, ginseng (*Panax ginseng* C.A. Meyer) has been used for medicinal purposes for a long time, and proponents for its use claim that ginseng extracts are effective in treating a wide range of disorders, including cancer [2–5]. Although the use of ginseng extracts for the treatment of prostate cancer can be questioned, it is now well established that there are many active compounds within a given ginseng extract that exhibit measurable anticancer effects [6–10]. It is not unreasonable to pursue the development and use of these active components for treatment of cancer, and our research team has an interest in developing selective ginsenosides for use in treatment of advanced prostate cancer.

From a nutraceutical perspective, this approach has been criticized in part because it can be argued that the therapeutic benefits arising from ginseng extracts are a result of the nutraceutical 'cocktail' that exists in the extract. It is suggested that the combination of active ingredients acts synergistically to produce therapeutic effects greater than that which can be achieved with single active components [11–14]. It is obviously difficult to address this without first establishing the activities of individual components and their metabolites. This work is complex and arduous, even if one assumed that all active components could be identified and isolated. Our approach has been to consider the development of isolated ginsenosides in combination with medicines that are a part of existing standards of care [14]. Here again, it is critical to first define the therapeutic effects achieved when the identified ginsenoside is used alone, before considering its use in combination with other chemotherapeutic drugs.

Our laboratory has recently reported on the antiprostate cancer activity of the ginsenoside Rh2 [15]. Rh2 is a

0959-4973 © 2012 Wolters Kluwer Health | Lippincott Williams & Wilkins DOI: 10.1097/CAD.0b013e32835006f5

triterpenoid glycoside saponin found in trace quantities in extracts from the roots of *P. ginseng* C.A. Meyer. However, it is one of the major *in vivo* metabolic products of ginseng when taken orally [16,17]. Others have demonstrated that Rh2 can be degraded, through a deglycosylation reaction, to aglycone protopanaxadiol (aPPD; Fig. 1a), and it has been suggested [18] that this degradation occurs in the intestine after oral administration of Rh2. Although we anticipated that treatment with Rh2 would result in systemic exposure to both Rh2 and aPPD, the liquid chromatography/mass spectrometry (LC/MS) methods used to assess the plasma concentration of these agents indicated that there was no detectable level of aPPD in the plasma or tissues extracted from Rh2-treated mice [15]. Further, as aPPD has been reported to exert its own therapeutic effects (including (a) inducing cell-cycle arrest in G [19], (b) inducing apoptosis [20,21] and/or autophagy [22,23], and (c) exhibiting antiestrogen activity [22]), it is important to characterize its effect when used as a single agent *in vivo*. The studies described here evaluate the pharmacokinetic and biodistribution behavior of aPPD formulated for oral administration. In addition, a preliminary assessment of treatment-induced toxicities and therapeutic activity was carried out. Overall, the research described here is significant and relevant to the development of aPPD as a therapeutic agent for castrate-resistant prostate cancer.

Methods

Test compounds and materials

Ginsenoside aglycone aPPD (molecular weight 460 g/mol), as a white powder, was purchased from LKT Laboratories Inc. (St Paul, Minnesota, USA) or was generously supplied by Panagin Pharmaceuticals Inc. (Richmond, British Columbia, Canada). Taxotere (docetaxel) was manufactured by Aventis Pharma Inc. (Saint-Laurent, Québec, Canada) and purchased from BC Cancer Agency Pharmacy (Vancouver, British Columbia, Canada) as a 40 mg/ml solution in polysorbate 80. Cholic acid (M.W. 408.58 g/mol) and all other chemicals were obtained from Sigma-Aldrich Canada Ltd (Oakville, Ontario, Canada).

Liquid chromatography/mass spectrometry analysis of aPPD

Instrumentation and conditions

The high-performance liquid chromatography (HPLC) system consisted of an integrated Waters Alliance 2695

Fig. 1

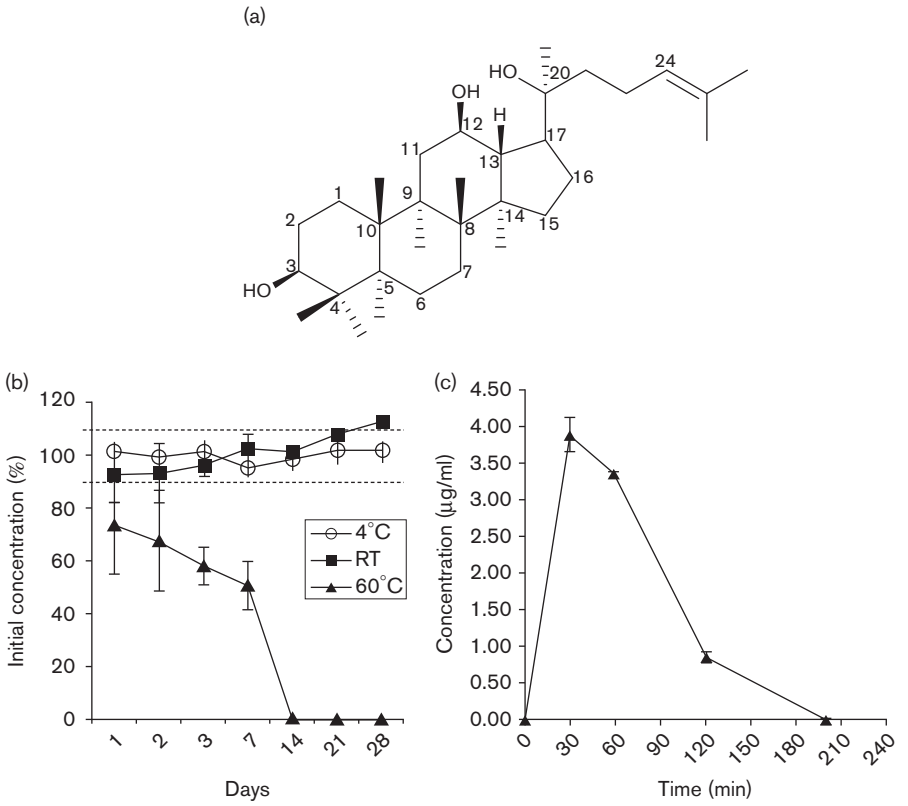

(a) Chemical structure of aglycone protopanaxadiol (aPPD). (b) Stability of aPPD in 100% ethanol for 28 days. Conditions are 4°C (empty circles), room temperature (RT, filled squares), and 60°C (filled triangles), $n=3$. (c) Mean plasma concentration–time profile of aPPD in mice after oral administration of 70 mg/kg; $n=3$ per time point.

quarternary solvent delivery system with low-pressure mixing, plus an autosampler and a 996 photodiode array detector (Waters Corp., Milford, Massachusetts, USA). aPPD and cholic acid were resolved on an Exterra C18 column (3.5 µm, 50 × 2.1 mm; Waters, Milford, Massachussets, USA) with mobile phases A, B, C, and D, double distilled water (ddH_2O), methanol, acetonitrile, and 0.5% acetic acid, respectively. The following gradient profile was used: $t = 0$–2 min, 40% A, 50% B, 10% D; $t = 3$–6 min, 10% A, 70% B, 10% C, 10% D; $t = 7$ min, 70% B, 20% C, 10% D; $t = 8$ min, 50% B, 40% C, 10% D; $t = 8.5$–9.0 min, 50% B, 50% C; $t = 10$–14 min, 100% C; $t = 15$–22 min, 40% A, 50% B, 10% D. The flow rate was 0.2–0.25 ml/min. A Waters/Micromass ZQ 2000 detector (Milford, Massachusetts, USA) was used for quantitative analysis of aPPD and cholic acid. The ZQ 2000 detector settings were as follows: capillary: 3 kV; desolvation temperature: 300°C; source temperature: 120°C; cone temperature: 20°C; extractor, RF lens, and multiplier voltages: 1.0, 0.5, and 650 V, respectively; and desolvation and cone gas flows: 350 and 50 l/h, respectively. For single ion recording functions, *m/z* of 519.01 and 407.2 were selected for aPPD and cholic acid, respectively, with 0.1 s dwell and cone voltages of 50 V. MassLynx version 3.4 (Micromass UK Ltd, Manchester, UK) was used to perform peak integration.

Solubility

To define the solubility of aPPD in ethanol, standard solutions of aPPD in ethanol were prepared at concentrations between 1 and 10 µmol/l (1, 2.5, 5, 7.5, and 10 µmol/l) and were analyzed in triplicate by HPLC. A calibration curve of peak area versus concentration was generated, and a linear relationship was seen. Three sets of saturated solutions of aPPD were then prepared at room temperature by incubating an excess of the compound in 2 ml of 100% ethanol. The mixture was mixed and stored at room temperature. After 30 min, material that was not dissolved precipitated in the tube. The amount of aPPD in the clear supernatant was quantified by HPLC.

Stability of samples at 4°C, at room temperature, and at 60°C

Stability studies were carried out by first preparing a solution of 120 mg of aPPD dissolved in 1.8 ml of 100% ethanol, a concentration based on the maximum solubility of 68.4 ± 10.0 mg/ml as determined using the methods described above. This solution was pipetted (200 µl) into each of nine Eppendorf tubes. One set of three tubes was stored at 4°C, at room temperature, and at 60°C. The concentration of aPPD in these solutions was determined by HPLC on days 1, 2, 3, 7, 14, 21, and 28.

Oral gavage formulation

We recently described a formulation methodology suitable for Rh2 [15], and this method was also used for aPPD. In brief, 120 mg of aPPD was dissolved and mixed in 1.8 ml of 100% ethanol (on the basis of a maximum solubility of 68.4 mg/ml). Subsequently, 700 µl of ddH_2O and 5.5 ml of propylene glycol were added and mixed. The resulting clear solution was then used for oral administration to mice. The highest daily dose of aPPD achievable using this formulation was 70 mg/kg, assuming a maximum gavage volume of not more than 150 µl.

Pharmacokinetic and biodistribution studies

Male nude mice (Harlan Sprague Dawley Inc.) that were 6–8 weeks old and weighing 25–31 g were randomly assigned to different treatment groups on the basis of their weight. Five groups of three mice each were dosed by oral gavage with aPPD at 70 mg/kg (117–145 µl) or with the vehicle control at an equivalent volume based on weight. Mice were killed by CO_2 asphyxiation, upon which blood (obtained by cardiac puncture) and major tissues (stomach, small intestine, liver, kidney, spleen, brain, and lung) were promptly collected 30, 60, 120, and 200 min after administration. Typically, 500–700 µl of blood was obtained and then placed into a Plasma Separator tube (Microtainer; Becton Dickinson, New Jersey, USA), mixed, and placed on ice. Tissues were collected and flash frozen before placing the samples in storage at –80°C. To assess aPPD extraction efficiencies, blank plasma and tissue homogenate samples (obtained from vehicle treated mice) were spiked with aPPD and cholic acid to obtain three concentrations (0.5, 2.0, and 10.0 µg/ml). The spiked samples were subsequently extracted and analyzed using the HPLC method described above.

Plasma: solid-phase sample preparation

C18 Sep-Pak extraction columns (Waters, Massachusetts, USA) mounted on a vacuum extraction manifold were first equilibrated with 1 ml of 100% methanol and 1 ml of ddH_2O. After loading with 200 µl of plasma spiked with 10 µl of cholic acid (internal standard), each column was subsequently washed with 1 ml of ddH_2O followed by 1 ml of 30% methanol. The column was then eluted twice with 1 ml of 100% methanol into Eppendorf tubes, and the eluate was dried in a speed-vac (Labconco Centrivap, Kansas City, Missouri, USA) at 35°C. The residue was reconstituted with 100 µl of 100% methanol, mixed vigorously, sonicated, and transferred into HPLC autosampler vials. A noncompartmental method using the nonlinear least squares regression program WinNonlin (Scientific Consulting Inc., Cary, North Carolina, USA) was used to analyze the plasma concentration data at four time points: 30, 60, 120, and 200 min. The area under the plasma concentration versus time curve (AUC) was calculated using the trapezoidal rule extrapolated to infinity. Pharmacokinetic parameters were generated, including the terminal half-life ($t_{1/2}$), the systemic clearance (Cl), the peak plasma concentration (C_{max}), and the time to reach C_{max} after oral administration (T_{max}).

Tissues

Tissue samples were ultrasonicated in 4 × w/v of 0.01 mol/l, pH 7.8, phosphate buffer. A volume of 200 µl of the homogenate was spiked with cholic acid (internal standard) and vortexed for 1 min. Ice-cold acetonitrile (800 µl) was added to the homogenate and vortexed for 1 min for protein precipitation. The sample was then centrifuged at 12 000 g for 15 min at 4°C. The supernatant was dried at 35°C, the residue was reconstituted in 200 µl of 100% methanol, vortexed and sonicated, and injected into the HPLC column. Standard calibration curves were analyzed at five concentrations ($n = 3$): 0.5, 2.0, 5.0, 10.0, and 20.0 µg/ml.

Efficacy and toxicity of aPPD

For efficacy studies, PC-3 cells (1.0×10^6) were inoculated subcutaneously into 6–8-week-old male nude mice (Harlan Sprague Dawley Inc., Indianapolis, Indiana, USA) weighing 25–31 g. After 14 days, tumors were measured and mice were then randomly assigned to different treatment groups. A caliper was used to measure each tumor, and the formula $V=(L\times W\times H)\frac{\pi}{6}$, where L is the length, W the width, and H is the height, was used to calculate the tumor volume. The average tumor volume when treatment was initiated was 120 mm^3. Four different treatment groups were defined: aPPD [70 mg/kg (117–145 µl volume range), oral QD × 5 schedule each week for 4 weeks], oral control consisting of ethanol : propylene glycol : water (2 : 7 : 1 ratio, 117–145 µl volume range, oral QD × 5 schedule each week for 4 weeks), docetaxel [positive control, 20 mg/kg (100–124 µl volume range), intravenously (i.v.) through the lateral tail vein, Q7D × 4 dose schedule], and saline [(100–124 µl volume range), i.v. Q7D × 4 dose schedule]. Mice were weighed 5 days a week, and tumors were measured twice a week for 25 days. For the aPPD and docetaxel groups the number of mice per group (n) was defined as eight, whereas six mice per group ($n = 6$) were used for the oral gavage and saline control groups. The mice were monitored daily for changes in weight and other signs of acute toxicity.

Analysis of apoptosis and proliferation markers

Upon completion of the efficacy studies, mice were killed and tumors were excised, formalin fixed, and paraffin embedded. A tissue microarray was constructed by extracting four 600-µm-diameter cores of tumor tissue from each paraffin block using a Beecher Instruments tissue core extractor (Sun Prairie, Wisconsin, USA) and re-embedding these cores into a gridded paraffin block. After construction, 4-µm tissue sections were cut and adhered to Fisher SuperFrost Plus glass slides (Fisher Scientific, Toronto, Ontario, Canada). Apoptotic cells were then visualized by terminal deoxynucleotidyl transferase (TdT)-mediated deoxyuridine triphosphate nick-end labeling staining, which was carried out using the ApopTag Peroxidase Kit (Millipore, Billerica, Massachusetts, USA). Tissues were pretreated with proteinase K for 15 min. Subsequently, the TdT enzyme was applied and the tissue was incubated in a humid chamber at 37°C for 1 h. The antidigoxigenin peroxidase conjugate was later applied for 30 min, followed by 3,3′-diaminobenzidine, and counter-staining was performed with hematoxylin and Staining Bluing Reagent. For Ki-67, a mouse-to-mouse immunohistochemical detection kit (Chemicon, Billerica, Massachusetts, USA) was used to decrease nonspecific staining. Ki-67 (Dako, Carpinteria, California, USA; 1 : 200) monoclonal antibodies were used in combination with immunoperoxidase procedures (labeled streptavidin biotin + peroxidase kit). Antigen retrieval was carried out by steaming with citrate buffer for 30 min. The TMA slides were imaged digitally and evaluated by visual scoring of apoptotic and Ki-67-positive cells. Scores from individual tumor cores with significant necrosis were omitted. Scoring was completed by two pathologists blinded to the study groups.

Statistical analysis

For each studied variable, mean and SEM were calculated. Statistical significance and differences between the described treatment groups were assessed using the Tukey–Kramer/Student t-tests by one-way analysis of variance. For these tests, the level of significance was set at a P-value of at least less than 0.05. All mean values were reported as mean ± SEM.

Results

Solubility, stability, and formulation in the ethanol–propylene glycol–water ternary solvent system

The maximum solubility of aPPD, as determined by LC/MS analysis of the supernatant of saturated solutions, was 68.4 ± 10.0 mg/ml. Stability results summarized in Fig. 1b suggest that aPPD is stable at 4°C and room temperature. LC/MS analysis of aPPD indicated that the drug concentration did not change over the 4-week time period. aPPD underwent rapid thermal degradation, measured as a loss of intact drug, at 60°C, with levels significantly decreasing to an undetectable level by week 2 (Fig. 1b). The rate constant for the observed decrease in concentration at 60°C, k (60°C), is 0.25, and the representative compound's half-life, $t_{1/2}$ (60°C), was estimated to be 7.0 days. A concentration change of ± 15% is generally considered acceptable in stability assays [23]; therefore, it was concluded that ethanol-solubilized drug solutions could be prepared and stored at 4°C for at least a time frame appropriate for the toxicity and efficacy assessments summarized below. Using the ethanol–propylene glycol–water ternary solvent system diagram designed by Sorby *et al.* [24], the dielectric constant of the ethanol, propylene glycol, and water mixture combined in a 2 : 7 : 1 v/v ratio was estimated to be approximately 31. The maximum solubility of aPPD was achieved at this 2 : 7 : 1 v/v ratio.

Pharmacokinetics and biodistribution

Extraction efficiencies for aPPD from mouse plasma and tissues at three different concentrations (0.5, 2.0, and

Table 1 Average extraction efficiencies of aPPD in plasma and tissues

Plasma (%)	Stomach (%)	Small intestine (%)	Liver (%)	Lung (%)	Spleen (%)	Kidney (%)	Brain (%)
59.0 ± 2.4	77.5 ± 4.7	94.9 ± 9.8	91.7 ± 6.9	89.7 ± 12.6	95.4 ± 12.4	104.6 ± 6.1	110.0 ± 2.7

Extraction standards were completed using three concentrations (0.5, 2.0, and 5.0 μg/ml) of aPPD, and each assay was carried out in triplicate.
aPPD, aglycone protopanaxadiol.

Table 2 Pharmacokinetic parameters for aPPD after oral administration of 70 mg/kg formulated in the ethanol–propylene glycol–water ternary solvent system described in Methods

Body weight (g)	$t_{1/2}$[a] (min)	C_{max}[b] (μg/ml)	T_{max}[c] (min)	Cl[d] (ml/min/kg)	AUC[e] (μg min/ml)
26.4 ± 2.9	28.5 ± 16.7	3.9 ± 1.4	40.0 ± 17.3	195.4 ± 32.4	330.7 ± 51.9

As $n=3$ per time point, three values were obtained for each parameter listed in the table.
aPPD, aglycone protopanaxadiol.
[a]Half-life.
[b]Peak concentration.
[c]Time to peak concentration.
[d]Clearance.
[e]Area under the plasma concentration vs. time curve.

10.0 μg/ml) were determined as described in the Methods, and the results are summarized in Table 1. The extraction efficiency from plasma was 59.0 ± 2.4% and this was not influenced by the concentration of aPPD used in these assays. Extraction efficiencies from tissues vary from 77.5 ± 4.7% in the stomach to essentially 100% in the kidney.

The plasma levels of aPPD determined at various time points after oral administration of aPPD have been summarized in Fig. 1c. Within 40 min of administration, aPPD levels in the plasma peaked at 3.9 ± 1.4 μg/ml, and after 200 min they were below the limit of quantitation (LOQ). Using these data, the pharmacokinetic parameters for aPPD were estimated, and are summarized in Table 2. The half-life ($t_{1/2}$) was 28.5 ± 16.7 min, the C_{max} was 3.9 ± 1.4 μg/ml, and the T_{max} was approximately 40.0 min. The clearance (Cl) was 195.4 ± 32.4 ml/min/kg and the AUC was 330.7 ± 51.9 μg min/ml.

Tissue distribution data have been summarized in Fig. 2a–e. As expected, given the route of administration, aPPD levels appeared to be highest in the stomach and small intestine 30 min after the gavage was administered, with approximately 44 and 32% of the drug recovered, respectively. Approximately 5% of the administered dose is found in the liver at the same time point. The aPPD level was quantifiable in the brain with 0.01% of the initial dose recovered at the 30-min time point. aPPD levels remained quantifiable in the stomach, small intestine, and liver 200 min after administration. The results clearly suggest that aPPD is bioavailable after oral gavage in the vehicle formulation.

In-vivo efficacy and toxicity

The therapeutic activity of aPPD was determined using mice bearing tumors established after subcutaneous injection of PC-3 human prostate cancer cells. This study included negative control groups (saline and the vehicle control), as well as a positive treatment control [docetaxel administered Q7D × 4 at an established therapeutic dose (maximum tolerated dose (MTD)]. The results summarized in Fig. 3a clearly show that aPPD [70 mg/kg (117–145 μl volume range), oral QD × 5 schedule each week for 4 weeks] was effective in inhibiting PC-3 tumor growth. At the end of the study (39 days after tumor cell inoculation and 25 days after treatment was initiated), the average tumor volume for saline (100–124 μl volume range, i.v. Q7D × 4 dose schedule)-treated and vehicle control (117–145 μl volume range, oral QD × 5 schedule each week for 4 weeks)-treated animals increased by approximately 200% from the time treatment was initiated. For animals treated with aPPD, the tumor volume increased by only 52% during this time course. The aPPD treatment group was statistically different from the control ($P = 0.0044$), saline ($P = 0.0159$), and docetaxel ($P = 0.0148$) groups. In comparison, docetaxel (20 mg/kg Q7D × 4) caused established PC-3 tumors to regress. By day 39, tumors in docetaxel-treated animals were still measurable, but had decreased by 75% from when treatment was initiated.

It should be noted that docetaxel administration was associated with almost 20% loss in body weight (Fig. 3b, filled squares), and this significant ($P = 0.0001$) weight loss compared with weight loss on saline administration is consistent with what would be expected for docetaxel administered at its MTD. In comparison, treatment with aPPD (Fig. 3b, filled triangles) resulted in less than 5% loss in mean body weight. This could be attributed to the repeated animal handling required for daily gavages as the vehicle alone (filled circle) engendered similar, albeit not significant, reductions in mean body weight.

PC-3 tumors were isolated from mice at the end of the study and prepared for immunohistochemical analysis of apoptosis and inhibition of Ki-67 labeling. The results, summarized in Fig. 3c–e, indicate that tumors from mice

Fig. 2

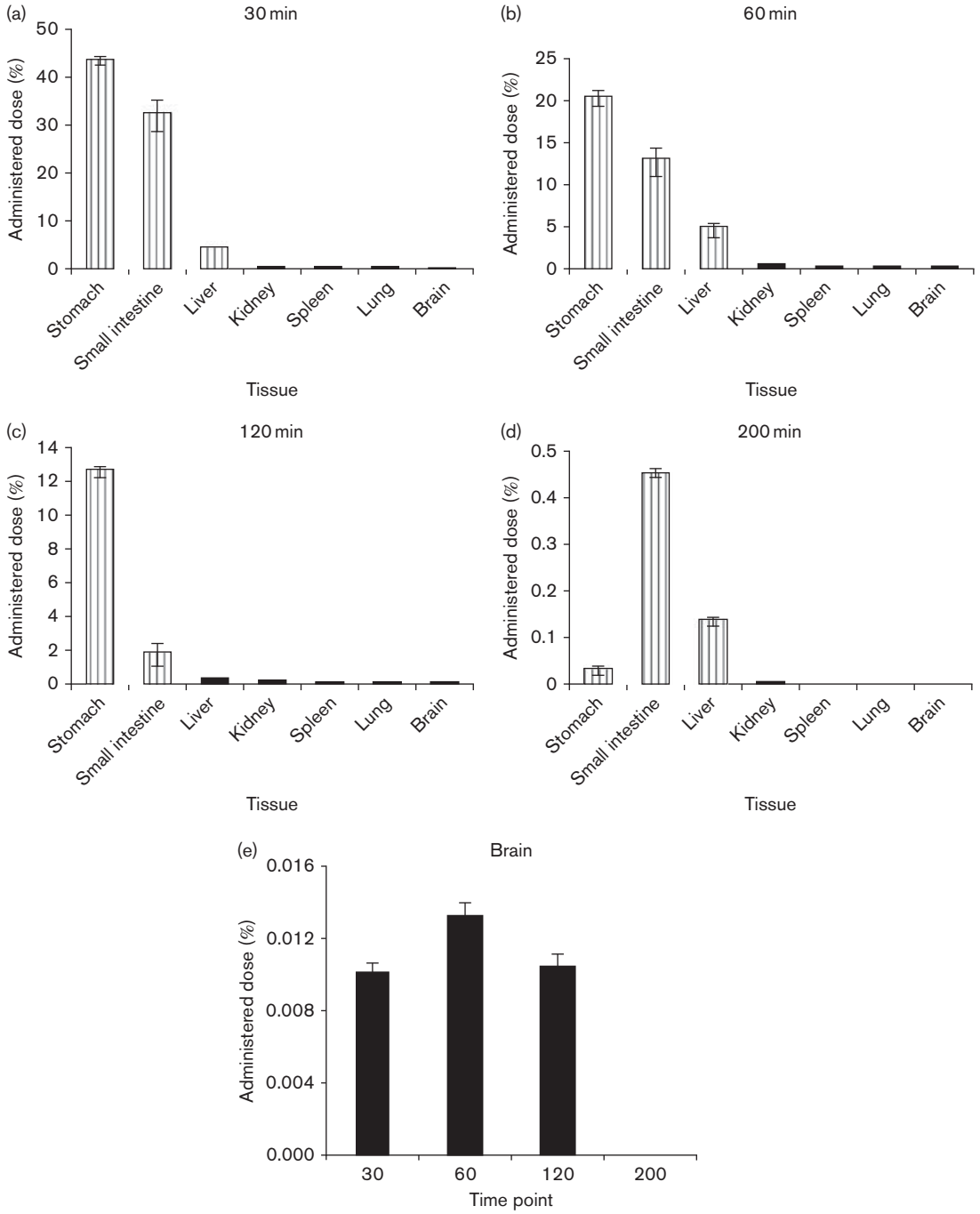

Administered dose (%) of aglycone protopanaxadiol in specified tissues isolated from mice after oral administration of 70 mg/kg. (a) 30 min, (b) 60 min, (c) 120 min, (d) 200 min. (e) Administered dose (%) of aPPD in the brain at 30, 60, 120, and 200 min time points. Results are expressed as mean values ± SEM. $n = 3$.

treated with docetaxel exhibited the highest apoptotic index. The average apoptotic index for the control was 9.30%. This increased to 15.6% in tumors from animals treated with aPPD and to 22.6% in tumors from animals treated with docetaxel. The apoptotic index observed in mice treated with docetaxel was significantly greater than that of control ($P = 0.0180$) but not significantly different from that observed in tumors from aPPD-treated animals ($P = 0.2305$). The apoptotic index in tumors from animals treated with aPPD was greater than that observed for controls, but this difference was not significantly different ($P = 0.0716$; Fig. 3d).

Fig. 3

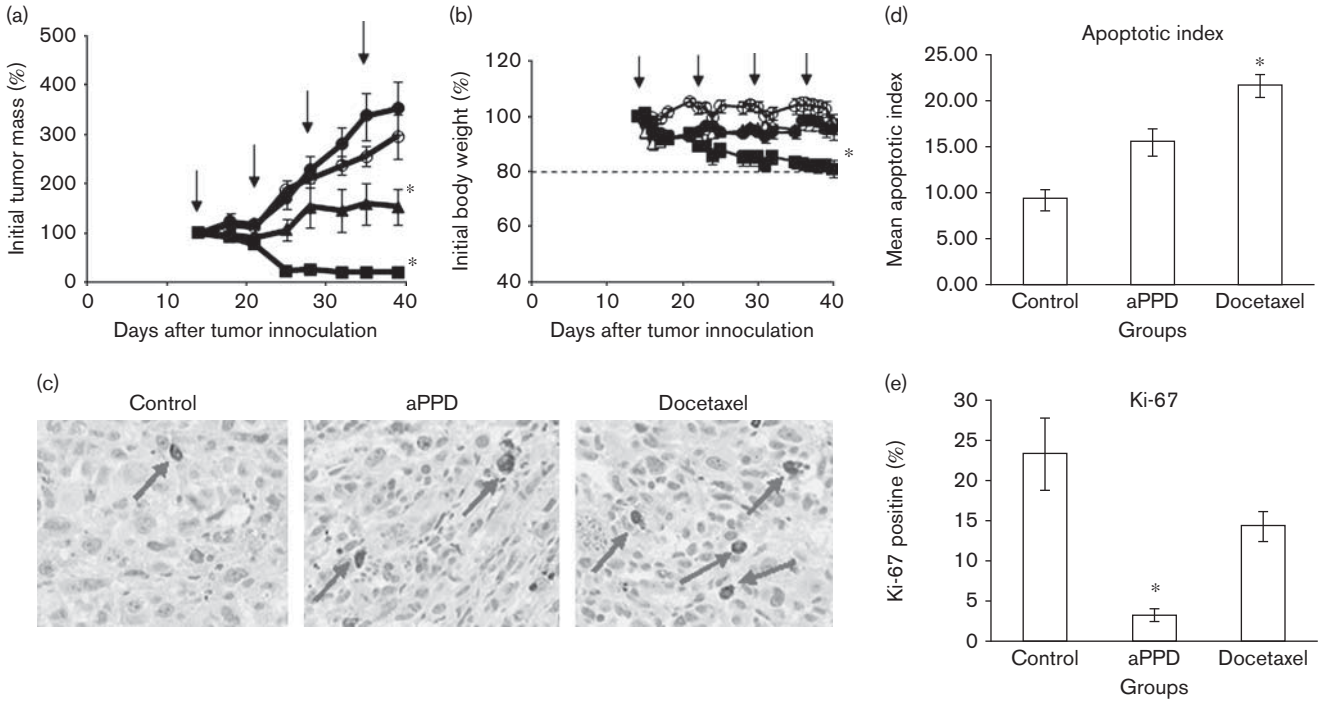

(a) In-vivo efficacy of aglycone protopanaxadiol (aPPD) in PC-3-bearing nude mice. Changes in tumor volume were followed up over time for animals treated with the oral gavage vehicle control (filled circles; ethanol, propylene glycol, and water), saline (empty circles), aPPD (70 mg/kg QD × 5; filled triangles), and docetaxel (20 mg/kg Q7D × 4; filled squares). Average tumor volumes are expressed as a percentage of the average initial tumor volume of each group at day 14, after inoculation of PC-3 cells. Mean value ± SEM is shown with error bars. A statistically significant difference was found between aPPD and control ($P = 0.0044$), saline ($P = 0.0159$), and docetaxel ($P = 0.0148$) groups on day 39. $n = 8$ for aPPD and docetaxel groups. $n = 6$ for oral gavage control and saline groups. (b) In-vivo toxicity as assessed by decrease in mean body weight. Body weight loss of greater than 20% is considered severe enough to warrant killing the animals. No animals showed any signs of toxicity other then weight loss in these studies. Mice administered docetaxel showed a significant weight loss compared with those administered saline ($P = 0.0001$). $n = 8$ for aPPD and docetaxel. $n = 6$ for the oral gavage control and saline groups. Mean value ± SEM is shown with error bars. (c) Representative tissue microarray spots for PC-3 tumors immunostained using a terminal deoxynucleotidyl transferase-mediated deoxyuridine triphosphate nick-end labeling assay. Apoptotic cells could be identified in areas of viable tissue, as indicated by arrows. (d) Apoptotic index summarized from ApopTag staining of tissue microarrays. (e) Summarized Ki-67 staining of tissue microarrays. Mean scores were determined as a percentage of the total number of cells. Four cores of tissue were extracted per tumor, as well as one tumor per animal. n (total number of cores) = 24 for the control and saline groups and 32 for aPPD and docetaxel groups. Mean value ± SEM is shown with error bars. *Signifies a statistically significant difference from the control.

Ki-67-positive cells identified in tumors from mice treated with aPPD were less abundant than those determined for the vehicle control or tumors derived from docetaxel-treated animals. Of the aPPD tumors, 3.2% were Ki-67 positive, whereas the control group exhibited a significantly higher level of 23.4% positive staining ($P = 0.0107$) and tumors from the docetaxel-treated groups exhibited 14.4% ($P = 0.007$) positive staining (Fig. 3e).

Discussion

We have shown that ginsenoside aPPD is a stable compound and have described a formulation suitable for oral administration. Pharmacokinetic data demonstrate that aPPD is absorbed when administered by oral gavage, and the systemic blood levels achieved are effective when used to treat mice bearing established PC-3 tumors. At the highest achievable dose (70 mg/kg), aPPD did not exhibit any toxicity in the nude mouse model used, and the systemic blood levels achieved after daily gavage were sufficient to inhibit growth of established PC-3 tumors. Biodistribution data indicated that intact aPPD could be isolated from several tissues after oral administration. In aggregate, the results presented here provide strong support for our efforts to develop aPPD for clinical evaluations, and we are particularly interested in the potential of using this agent in combination with docetaxel for treatment of relapsed and hormone-insensitive metastatic prostate cancer. The discussion here will therefore consider the potential of aPPD and its appropriate formulation for use as a well-tolerated drug with potential to augment the therapeutic effects of current chemotherapy.

Although we are interested in the development of systemic formulations for aPPD, the focus here was to define a suitable formulation for oral administration. aPPD (Fig. 1a) is an extremely hydrophobic molecule and presents some formulation challenges as the hydrocarbon

skeleton of the steroid exerts a powerful hydrophobic influence on its solubility in water and ethanol. Compounds that are largely hydrophobic have a greater preference for solvents with low or zero dipole moments and dielectric constants. Ethanol, however, with a dielectric constant of 24.6 is a better solvent for aPPD compared with water, which possesses a dielectric constant of 80.1 [25]. Ethanol was used to dissolve aPPD at a concentration of 68.4 mg/ml, and this solubilized material was then mixed with propylene glycol and water to define an oral dosage formulation. As noted in Fig. 1b, accelerated stability studies with aPPD in ethanol at three temperatures suggested that aPPD could be stored at 4°C or at room temperature for at least 1 month without any significant change in concentration. With a boiling point of 78.15°C for ethanol [26], we also chose to evaluate the stability of aPPD at 60°C, maintaining the samples in sealed vials to minimize evaporation. aPPD was unstable when incubated at this higher temperature. Degradation was observed within 48 h and progressed rapidly with complete degradation within 14 days.

The final formulation selected for use in oral aPPD administration comprised ethanol, propylene glycol, and water mixed at a ratio (v : v) of 2 : 7 : 1. Propylene glycol is extensively used both as a solvent for water-insoluble drugs and as a preservative in topical, parenteral, and oral formulations [27]. Propylene glycol has been shown to be relatively innocuous ($LD_{50} = 21$ g/kg) in acute oral toxicity studies using rats [27,28]. Using the ethanol–propylene glycol–water ternary solvent system diagram designed by Sorby *et al.* [24], the dielectric constant of the formulated aPPD oral gavage mixture was estimated to be 31, ideal for the solubility of aPPD. In addition to defining a suitable formulation for use in in-vivo studies, it was essential to have appropriate analytical methods in place to help assess drug stability, as well as aPPD pharmacokinetic and biodistribution behavior after administration. Therefore, a significant portion of the work described here concerns the development and partial validation of an analytical assay for aPPD. As summarized earlier, the limit of detection was estimated to be 5.0 ng/ml, whereas the LOQ value was 20.0 ng/ml. Xie *et al.* [29] obtained an LOQ of 2 ng/ml for Rh2, the corresponding glycosylated ginsenoside of aPPD, in rat plasma and estimated that plasma concentrations of Rh2 could be reliably quantified between 2 and 100 ng/ml. The mobile phase used by these investigators was supplemented with ammonium chloride. Using the method developed here, we previously obtained a limit of detection and LOQ of 2.0 and 5.0 ng/ml, respectively, for Rh2 [15], thus demonstrating that this method can be used reliably for the determination of aPPD in mouse plasma and tissues. The robustness of our method is evidenced by the linearity of the tissue calibration curves, with an excellent correlation factor of 0.97 (data not shown).

Using the LC/MS assay described above, pharmacokinetic studies were completed after oral administration of aPPD in the vehicle control. The data summarized in Fig. 1c clearly show that aPPD is bioavailable after oral gavage. These results are consistent with a previous study of Rh2 and ginsenoside K, two ginsenosides sharing a similar aglycone structure with aPPD. After oral administration, these two ginsenosides reach a T_{max} of 30 min in the plasma compartment [15,30]. We have obtained a T_{max} of 40 min for aPPD. aPPD is more hydrophobic than both Rh2 and compound K, which have a sugar moiety attached to their steroidal structure. aPPD has half the solubility of Rh2 in 100% ethanol (68.4 mg/ml) and is close to insoluble in water. Our results indicate that aPPD is retained in the gastrointestinal tract at significant levels for at least 2 h after administration. The higher hydrophobicity of aPPD is probably the most significant contributor to its more extended retention in the gastrointestinal tract. As shown in Fig. 2a, only 5% of the administered dose reached the liver 30 min after administration, compared with 28% for Rh2 [15]. As the pH in the small intestine of mice varies between 6.5 and 7.1 [31], we suspect that aPPD is poorly absorbed here, despite its lipophilicity, because it has been shown to be optimally transported by Caco-2 cells at a pH of 8.0 [32]. Our results assessing tissue levels of aPPD after oral gavage suggest that aPPD can cross the blood–brain barrier. It is established that lipophilic drugs penetrate the endothelial cells of the blood–brain barrier more easily than do hydrophobic drugs [33], and passive diffusion permeation rates are correlated to lipophilicity [34]. In addition to its lipophilicity, we can speculate that the accumulation of aPPD in the brain is the result of its effectiveness in stimulating breast cancer resistance protein (BCRP)-ATPase activity after BCRP inhibition, which would allow it to be transported by BCRP across the blood–brain barrier [16]. The biodistribution data presented here are consistent with the conclusion that aPPD administered orally in the ethanol, propylene glycol, and water formulation is readily absorbed and accesses key target tissues in an intact, unmetabolized form.

Importantly, the formulation developed here was well tolerated when given (70 mg/kg) QD × 5 each week for 4 weeks. The mice monitored in our study showed no acute signs of toxicity as determined by body weight loss (Fig. 3b), and this observation is consistent with other studies [35] that suggest that ginsenosides and their aglycones cause negligible toxicity, even at the maximal achievable dose. As mice that we previously treated with Rh2 also did not show acute signs of toxicity [15], it could be suggested that aPPD and Rh2, both members of the 20(*S*)-protopanaxadiol ginsenoside category, share a similar toxicity profile. Secondary measurements of liver and kidney toxicities after Rh2 administration in nude mice showed no increase in serum alanine aminotransferase and aspartate aminotransferase activities, and serum creatinine levels were not statistically different from

serum creatinine levels of the control group, suggesting no significant toxic effects of Rh2 on these organs [15]. Similar conclusions can be anticipated for aPPD.

aPPD appears to exhibit therapeutic activity when used to treat established tumors derived after subcutaneous injection of PC-3 cells (Fig. 3a), and the results suggest that the activity, albeit lower than docetaxel administered at its MTD, was significantly different from the activity of control ($P = 0.0044$) and saline ($P = 0.0159$) groups. To better understand the nature of aPPD-mediated therapeutic effects, PC-3 tumors were isolated at the end of the treatment phase of the study and apoptosis (TdT-mediated deoxyuridine triphosphate nick-end labeling staining) and proliferation (Ki-67) were measured. The apoptotic index of the docetaxel group was significantly higher than the apoptotic index of the control ($P = 0.0180$). Although the value determined in tumors from animals treated with aPPD were greater than that seen for control tumors, this difference was not statistically different ($P = 0.0716$; Fig. 3d). Others have shown that aPPD and other ginsenoside aglycones are strong promoters of apoptosis [19,36]. The fact that we did not observe significant increases in the apoptotic index may be related to the time points used in our study. In our study, we demonstrated that aPPD significantly inhibited cell proliferation, as measured by Ki-67 labeling (Fig. 3e), and the extent of suppression was significantly lower than that observed in tumors isolated from animals treated with docetaxel ($P = 0.007$).

In summary, the formulation that we describe here is well tolerated and effective when used to treat established PC-3 tumors. Pharmacokinetic and biodistribution studies suggest that aPPD is well absorbed. Future studies will assess the activity of this ginsenoside when used in combination with conventional cytotoxic/cytostatic drugs, in particular docetaxel. The efficacy results shown here indicate that continuous dosing of aPPD will mediate effects that suppress tumor growth (i.e. result in stable disease), but it is understood that tumor growth will recur once treatment is stopped. This cytostatic effect may be important when using aPPD in a combination setting with a chemotherapeutic agent known to cause regression of established tumors, as was observed here when PC-3 tumor-bearing mice were treated with docetaxel.

Acknowledgements

The authors thank Panagin Pharmaceuticals Inc., Richmond, BC, Canada, for generously supplying aPPD. They also acknowledge the staff of the Jack Bell Animal Resource Centre for providing outstanding care for the animals used in these studies.

This research was supported in part by grants from the Canadian Institutes of Health Research (M.B.B.) and Health Canada (E.G.).

Conflicts of interest

There are no conflicts of interest.

References

1 Richardson MA, Sanders T, Palmer JL, Greisinger A, Singletary SE. Complementary and alternative medicine use in a comprehensive cancer center and the implications for oncology. *J Clin Oncol* 2000; **18**:2505–2514.
2 Nah SY, Park HJ, McCleskey EW. A trace component of ginseng that inhibits Ca^{2+} channels through a pertussis toxin-sensitive G protein. *Proc Natl Acad Sci USA* 1995; **92**:8739–8743.
3 Yun TK, Lee YS, Lee YH, Kim SI, Yun HY. Anticarcinogenic effect of Panax ginseng C.A. Meyer and identification of active compounds. *J Korean Med Sci* 2001; **16 (Suppl)**:S6–S18.
4 Zhang D, Yasuda T, Yu Y, Zheng P, Kawabata T, Ma Y, *et al*. Ginseng extract scavenges hydroxyl radical and protects unsaturated fatty acids from decomposition caused by iron-mediated lipid peroxidation. *Free Radic Biol Med* 1996; **20**:145–150.
5 Duda RB, Zhong Y, Navas V, Li MZ, Toy BR, Alavarez JG. American ginseng and breast cancer therapeutic agents synergistically inhibit MCF-7 breast cancer cell growth. *J Surg Oncol* 1999; **72**:230–239.
6 Kim HE, Oh JH, Lee SK, Oh YJ. Ginsenoside RH-2 induces apoptotic cell death in rat C6 glioma via a reactive oxygen- and caspase-dependent but Bcl-X(l)-independent pathway. *Life Sci* 1999; **65**:PL33–PL40.
7 Fei XF, Wang BX, Tashiro S, Li TJ, Ma JS, Ikejima T. Apoptotic effects of ginsenoside Rh2 on human malignant melanoma A375-S2 cells. *Acta Pharmacol Sin* 2002; **23**:315–322.
8 Oh M, Choi YH, Choi S, Chung H, Kim K, Kim SI, *et al*. Anti-proliferating effects of ginsenoside Rh2 on MCF-7 human breast cancer cells. *Int J Oncol* 1999; **14**:869–875.
9 Park JA, Lee KY, Oh YJ, Kim KW, Lee SK. Activation of caspase-3 protease via a Bcl-2-insensitive pathway during the process of ginsenoside Rh2-induced apoptosis. *Cancer Lett* 1997; **121**:73–81.
10 Kim YS, Jin SH, Lee YH, Park JD, Kim SI. Differential expression of protein kinase C subtypes during ginsenoside Rh2-Induced apoptosis in SK-N-BE(2) and C6Bu-1 cells. *Arch Pharm Res* 2000; **23**:518–524.
11 Frei E. Principles of dose, schedule and combination chemotherapy. In: Kufe D, Holland J, Frei E, editors. *Cancer medicine*. **6**: Hamilton, Ontario: BC Decker Inc.; 2003. pp. 669–677.
12 Chou TC, Talalay P. Quantitative analysis of dose-effect relationships: the combined effects of multiple drugs or enzyme inhibitors. *Adv Enzyme Regul* 1984; **22**:27–55.
13 Budman DR, Calabro A, Kreis W. Synergistic and antagonistic combinations of drugs in human prostate cancer cell lines in vitro. *Anticancer Drugs* 2002; **13**:1011–1016.
14 Xie X, Eberding A, Madera C, Fazli L, Jia W, Goldenberg L, *et al*. Rh2 synergistically enhances paclitaxel or mitoxantrone in prostate cancer models. *J Urol* 2006; **175**:1926–1931.
15 Musende AG, Eberding A, Wood C, Adomat H, Fazli L, Hurtado-Coll A, *et al*. Pre-clinical evaluation of Rh2 in PC-3 human xenograft model for prostate cancer in vivo: formulation, pharmacokinetics, biodistribution and efficacy. *Cancer Chemother Pharmacol* 2009; **64**:1085–1095.
16 Jin J, Shahi S, Kang HK, Hendrik WVV, Fan T. Metabolites of ginsenosides as novel BCRP inhibitors. *Biochem Biophys Res Commun* 2006; **345**:1308–1314.
17 Popovich DG, Kitts DD. Generation of ginsenosides Rg3 and Rh2 from North American ginseng. *Phytochemistry* 2004; **65**:337–344.
18 Bae EA, Han MJ, Kim EJ, Kim DH. Transformation of ginseng saponins to ginsenoside Rh2 by acids and human intestinal bacteria and biological activities of their transformants. *Arch Pharm Res* 2004; **27**:61–67.
19 Popovich DG, Kitts DD. Structure-function relationship exists for ginsenosides in reducing cell proliferation and inducing apoptosis in the human leukemia (THP-1) cell line. *Arch Biochem Biophys* 2002; **406**:1–8.
20 Wang W, Wang H, Rayburn ER, Zhao Y, Hill DL, Zhang R. 20(S)-25-methoxyl-dammarane-3beta, 12beta, 20-triol, a novel natural product for prostate cancer therapy: activity in vitro and in vivo and mechanisms of action. *Br J Cancer* 2008; **98**:792–802.
21 Liu GY, Bu X, Yan H, Jia WW. 20S-protopanaxadiol-induced programmed cell death in glioma cells through caspase-dependent and -independent pathways. *J Nat Prod* 2007; **70**:259–264.
22 Yu Y, Zhou Q, Hang Y, Bu X, Jia W. Antiestrogenic effect of 20S-protopanaxadiol and its synergy with tamoxifen on breast cancer cells. *Cancer* 2007; **109**:2374–2382.
23 USP C. *USP Pharmacopeia & National Formulary*. Rockville, MD: Board of Trustees of the USP Pharmacopeial Convention, Inc.; 2000.

24 Sorby DL, Bitter RG, Webb JG. Dielectric constants of complex pharmaceutical solvent systems. I. Water–ethanol–glycerin and water–ethanol–propylene glycol. *J Pharm Sci* 1963; **52**:1149–1153.

25 James KC. *Solubility and related properties*. New York: M. Dekker; 1986.

26 O'Neil MJ, Smith A, Heckelman PE, Obenchain JR, Gallipeau JAR, D'Arecca MA. *The Merck Index*. 13th ed. Whitehouse Station, NJ: Merck Research Laboratories; 2001.

27 Nagatomo I, Akasaki Y, Hashiguchi W, Tominaga M, Uchida M, Takigawa MA. Solvent used for antiepileptic drugs increases serum and brain zonisamide concentrations in seizure-susceptible EL mice. *Epilepsy Behav* 2001; **2**:357–362.

28 Lanigan RS. Final report on the safety assessment of PPG-11 and PPG-15 stearyl ethers. *Int J Toxicol* 2001; **20**:53–59.

29 Xie HT, Wang GJ, Sun JG, Tucker I, Zhao XC, Xie YY, *et al*. High performance liquid chromatographic-mass spectrometric determination of ginsenoside Rg3 and its metabolites in rat plasma using solid-phase extraction for pharmacokinetic studies. *J Chromatogr B Analyt Technol Biomed Life Sci* 2005; **818**:167–173.

30 Akao T, Kanaoka M, Kobashi K. Appearance of compound K, a major metabolite of ginsenoside Rb1 by intestinal bacteria, in rat plasma after oral administration – measurement of compound K by enzyme immunoassay. *Biol Pharm Bull* 1998; **21**:245–249.

31 Kararli TT. Comparison of the gastrointestinal anatomy, physiology, and biochemistry of humans and commonly used laboratory animals. *Biopharm Drug Dispos* 1995; **16**:351–380.

32 Xie HT, Wang GJ, Chen M, Jiang XL, Li H, Lu H, *et al*. Uptake and metabolism of ginsenoside Rh2 and its aglycon protopanaxadiol by Caco-2 cells. *Biol Pharm Bull* 2005; **28**:383–386.

33 Rapoport SI, Ohno K, Pettigrew KD. Drug entry into the brain. *Brain Res* 1979; **172**:354–359.

34 Levin VA. Relationship of octanol/water partition coefficient and molecular weight to rat brain capillary permeability. *J Med Chem* 1980; **23**:682–684.

35 Chen SE, Sawchuk RJ, Staba EJ. American ginseng. III. Pharmacokinetics of ginsenosides in the rabbit. *Eur J Drug Metab Pharmacokinet* 1980; **5**:161–168.

36 Wang W, Rayburn ER, Hao M, Zhao Y, Hill DL, Zhang R, *et al*. Experimental therapy of prostate cancer with novel natural product anti-cancer ginsenosides. *Prostate* 2008; **68**:803–918.